Ann Nucl Med (2013) 27:314–324
DOI 10.1007/s12149-013-0687-7

ORIGINAL ARTICLE

Biological evaluation of 3-[^{18}F]fluoro-α-methyl-D-tyrosine (D-[^{18}F]FAMT) as a novel amino acid tracer for positron emission tomography

Yasuhiro Ohshima · Hirofumi Hanaoka · Hideyuki Tominaga · Yoshikatsu Kanai · Kyoichi Kaira · Aiko Yamaguchi · Shushi Nagamori · Noboru Oriuchi · Yoshito Tsushima · Keigo Endo · Noriko S. Ishioka

Received: 12 March 2012 / Accepted: 8 January 2013 / Published online: 23 January 2013

Abstract
Objective 3-[^{18}F]Fluoro-α-methyl-L-tyrosine (L-[^{18}F]FAMT) is a useful amino acid tracer for positron emission tomography (PET) imaging of malignant tumors. Because D-amino acids are not well distributed in non-target organs and are rapidly excreted in urine, the D-isomer of [^{18}F]FAMT could allow clear PET imaging of tumors early after administration. In this study, we prepared 3-[^{18}F]fluoro-α-methyl-D-tyrosine (D-[^{18}F]FAMT) and evaluated its usefulness.
Methods D-[^{18}F]FAMT was synthesized according to the method for preparation of L-[^{18}F]FAMT. The in vitro and in vivo stability of [^{18}F]FAMT were evaluated by high-performance liquid chromatography. Cellular uptake of [^{18}F]FAMT was evaluated using LS180 colon adenocarcinoma cells. Biodistribution studies were performed in LS180 tumor-bearing mice, and the tumors were imaged using a small-animal PET scanner.
Results The radiolabeling yield of D-[^{18}F]FAMT was approximately 10 %, similar to that of L-[^{18}F]FAMT. Over 95 % of D-[^{18}F]FAMT remained intact in mice until 60 min after administration. D-[^{18}F]FAMT was gradually taken up by the LS180 cells. Tumor uptake of D-[^{18}F]FAMT was competitively inhibited by pretreatment with α-methyl-L-tyrosine, a selective substrate for the system L-amino acid transporter 1 (LAT1), suggesting the involvement of LAT1 in tumor uptake of D-[^{18}F]FAMT. In biodistribution studies, D-[^{18}F]FAMT showed rapid clearance from the blood, marked accumulation and retention in the tumor, and lower accumulation in non-target organs, especially kidney and pancreas, compared to L-[^{18}F]FAMT. The amount of D-[^{18}F]FAMT in the tumor was also reduced, and tumor-to-blood ratio and tumor-to-muscle ratio of D-[^{18}F]FAMT were similar to those of L-[^{18}F]FAMT at every time point. PET imaging with D-[^{18}F]FAMT did not provide a clear image of the tumor early after administration. However, D-[^{18}F]FAMT

Y. Ohshima (✉) · N. S. Ishioka
Medical Radioisotope Application Group, Quantum Beam Science Directorate, Japan Atomic Energy Agency, 1233 Watanuki, Takasaki, Gunma 370-1292, Japan
e-mail: ohshima.yasuhiro@jaea.go.jp

H. Hanaoka
Department of Molecular Imaging and Radiotherapy, Graduate School of Pharmaceutical Sciences, Chiba University, Inohana, Chuo-ku, Chiba 260-8675, Japan

H. Tominaga
Department of Molecular Imaging, Graduate School of Medicine, Gunma University, Showa-machi, Maebashi, Gunma 371-8511, Japan

Y. Kanai · S. Nagamori
Division of Bio-system Pharmacology, Graduate School of Medicine, Osaka University, Suita, Osaka 565-0871, Japan

K. Kaira
Department of Medicine and Molecular Science, Graduate School of Medicine, Gunma University, Showa-machi, Maebashi, Gunma 371-8511, Japan

A. Yamaguchi
Department of Bioimaging Information Analysis, Graduate School of Medicine, Gunma University, Showa-machi, Maebashi, Gunma 371-8511, Japan

N. Oriuchi · Y. Tsushima · K. Endo
Department of Diagnostic Radiology and Nuclear Medicine, Graduate School of Medicine, Gunma University, Showa-machi, Maebashi, Gunma 371-8511, Japan

provided higher tumor-to-background contrast than L-[^{18}F]FAMT.

Conclusions D-[^{18}F]FAMT showed rapid blood clearance, low accumulation in non-target organs, and tumor-selective imaging compared with L-[^{18}F]FAMT. Thus, D-[^{18}F]FAMT could potentially serve as a novel PET tracer for imaging malignant tumors.

Keywords 3-[^{18}F]Fluoro-α-methyl-L-tyrosine (L-[^{18}F]FAMT) · 3-[^{18}F]Fluoro-α-methyl-D-tyrosine (D-[^{18}F]FAMT) · Positron emission tomography (PET) · Amino acid tracer · Tumor

Introduction

Radiotracers that enable the visualization of abnormal tumor metabolism are useful tools for tumor diagnosis, and many tracers have been developed and used for clinical diagnosis [1]. 2-[^{18}F]Fluoro-2-deoxy-D-glucose ([^{18}F]FDG) is most widely used for tumor imaging in positron emission tomography (PET) [1, 2]. However, high levels of accumulation in non-target tissues such as brain and inflammatory sites often impede the accuracy of PET in diagnosing tumors [2]. Amino acid tracers usually show low accumulation in non-target tissues compared to [^{18}F]FDG, and they are favorable tracers in terms of tumor selectivity [1, 3]. At present, several amino acid tracers, including [^{11}C]methionine and ^{18}F-labeled L-tyrosine analogs, have been introduced into clinical practice and have been used to visualize malignant tumors in patients [1–5].

Further, 3-[^{18}F]fluoro-α-methyl-L-tyrosine (L-[^{18}F]FAMT) is a useful amino acid tracer, and it is selectively accumulated in tumors without incorporation in protein synthesis [6, 7]. Clinical studies have shown that L-[^{18}F]FAMT can be used to differentiate between benign lesions and malignant tumors [8, 9]. L-[^{18}F]FAMT has shown higher specificity than [^{18}F]FDG with regard to the detection of maxillofacial tumors, thoracic tumors, and lymph node metastases of non-small cell lung cancer [10–12]. L-[^{18}F]FAMT is transported into tumor cells solely through amino acid transport systems, and in particular, the involvement of system L-amino acid transporter 1 (LAT1) has been suggested [10, 13–15]. LAT1 is a major nutrient transport system responsible for Na^+-independent transport of large neutral amino acids including branched and aromatic amino acids [16–18]. LAT1 is also known to be widely expressed in human cancers and cancer cell lines, where it has been shown to play essential roles in growth and survival [19].

L-[^{18}F]FAMT exhibits slower clearance from the blood than [^{18}F]FDG with high accumulation and retention in the kidney, possibly hindering diagnostic accuracy. However, L-amino acids have corresponding D-isomers that have some favorable properties for the development of PET tracers. Since mammals rarely use D-amino acids for their biological activity, D-amino acids would not be taken up by the normal tissues. In addition, D-amino acids are rapidly cleared from the circulation and highly excreted in the urine compared with L-isomers [20, 21]. Previous studies reported that radiolabeled D-amino acid showed rapid clearance from the blood and provided clear PET images of tumors [22]. Thus, we expected the D-isomer of FAMT to allow clear PET imaging of a tumor early after administration. In this study, we synthesized D-[^{18}F]FAMT and evaluated its usefulness as a novel PET tracer. In addition, we investigated the mechanism of tumor uptake of D-[^{18}F]FAMT both in vitro and in vivo.

Materials and methods

Generals

Alpha-methyl-L-tyrosine, 2-aminobicyclo[2.2.1]heptane-2-carboxylic acid (BCH), 2-(methylamino)isobutyric acid (MeAIB), and dimethyl sulfoxide (DMSO) were purchased from Sigma-Aldrich (St Louis, MO, USA). Alpha-methyl-D-tyrosine was purchased from IRIS Biotech (Marktredwitz, Germany). Dulbecco's modified Eagle's medium, penicillin, streptomycin, Hank's balanced salt solution (HBSS), and L-tyrosine were purchased from Wako Pure Chemical Industries (Osaka, Japan). Fetal bovine serum was purchased from AusGeneX (Santa Clara, CA, USA). Male ddY mice were purchased from Japan SLC (Hamamatsu, Japan), and male BALB/c (nu/nu) mice were purchased from CLEA Japan (Tokyo, Japan). All other chemicals used were of the highest purity available.

Production of D- or L-[^{18}F]FAMT

Positron-emitting fluorine ($^{18}F_2$) was produced by a $^{20}Ne(d,\alpha)^{18}F$ nuclear reaction using the biomedical cyclotron CYPRIS HM-18 (HM-18; Sumitomo Heavy Industries Ltd., Tokyo, Japan). L- and D-[^{18}F]FAMT were synthesized according to the method developed by Tomiyoshi et al. [6]. Briefly, α-methyl-L-tyrosine and α-methyl-D-tyrosine were fluorinated by [^{18}F]acetyl hypofluoride, and separation and purification were performed by a remote control system. Separation of [^{18}F]FAMT was carried out by high-performance liquid chromatography (HPLC): column, LiChrosorb RP-18 10 mm internal diameter (ID) × 250 mm, 10 μm particle size; column temperature, 25 °C; mobile phase, methanol/0.1 % acetic acid = 1/9; flow rate, 6 ml/min; detection, absorbance at 280 nm and radioactivity. Retention times of D- or L-[^{18}F]FAMT and their 2-fluoroisomers

were 7.4 and 6.4 min, respectively. The radiochemical purity of [^{18}F]FAMT was analyzed using the following HPLC conditions: column, LiChrosorb RP-18, 4.6 mm ID × 250 mm, 10 mm particle size and Inertsil ODS-3, 4.6 mm ID × 150 mm, 5 mm particle size; column temperature, 25 °C; mobile phase, methanol/0.1 % acetic acid = 1/9; flow rate, 2 ml/min; detection, absorbance at 280 nm and radioactivity (radiodetectors, Universal Giken, Odawara, Japan). Retention times of D- and L-[^{18}F]FAMT were 4.5 min with LiChrosorb RP-18 and 3.0 min with Inertsil ODS-3. Enantiomeric purity of D- or L-[^{18}F]FAMT was analyzed after fractionation by the following conditions: column, CHIRALPAK MA (+), 4.6 mm ID × 50 mm, 10 μm particle size; column temperature, 25 °C; mobile phase, 0.25 mM cupric sulfate solution; flow rate, 0.5 ml/min; detection, absorbance at 280 nm and radioactivity. The retention times of D-[^{18}F]FAMT and L-[^{18}F]FAMT were 50 and 75 min, respectively. Non-radioactive D- or L-FAMT was synthesized by direct fluorination of α-methyl-D-tyrosine or α-methyl-L-tyrosine, using fluorine gas according to the method developed by Tomiyoshi et al. [6], and identified by ^{1}H-NMR analysis [400 MHz, D_2O/DCl, L-FAMT: δ (ppm) 1.39 (3H, s), 2.76 (1H, d, J = 14.0 Hz), 3.08 (1H, d, J = 14.0 Hz), 6.76–6.90 (3H, m); D-FAMT: δ (ppm) 1.39 (3H, s), 2.76 (1H, d, J = 14.0 Hz), 3.08 (1H, d, J = 14.0 Hz), 6.76–6.90 (3H, m)] and optical rotation [L-FAMT: [α](25, D) = −10.9 (deg) (c = 0.05, 1 N HCl), D-FAMT: [α](25, D) = 10.6 (deg) (c = 0.1)]. For the measurement of optical rotation, FAMT was dissolved in ultrapure water at a concentration of 0.05 g/100 ml.

In vitro and in vivo stability

The animals were cared for and treated in accordance with the guidelines of the animal care and experimentation committee at our facility. For the evaluation of in vitro stability, 20 μl of D- or L-[^{18}F]FAMT (1 MBq) was added to 180 μl of freshly prepared murine plasma or human plasma (Kohjin Bio, Saitama, Japan), and the solution was incubated at 37 °C for 1, 3, and 6 h. After filtration through a 10-kDa cutoff ultrafiltration membrane (Vivaspin 500; Sartorius, Goettingen, Germany), the radioactivity of the sample was analyzed by HPLC with the Inertsil ODS-3 column. For the evaluation of in vivo stability, blood was collected from normal ddY mice at 10, 30, and 60 min after administration of D- or L-[^{18}F]FAMT (20 MBq/head). After centrifugation at 5,000 rpm for 5 min at 4 °C, the resultant serum samples were filtered through a 10-kDa cutoff ultrafiltration membrane. The radioactivity of the sample was analyzed by HPLC as described above. The fraction of D- or L-[^{18}F]FAMT was expressed as a percentage of the total radioactivity in the sample.

Cellular uptake studies

A human colon adenocarcinoma cell line, LS180, was purchased from the American Type Culture Collection (Manassas, VA, USA) and routinely maintained in Dulbecco's modified Eagle's medium containing 10 % heat-inactivated fetal bovine serum, penicillin (100 U/ml), streptomycin (100 μg/ml) and L-glutamine (2 mM) at 37 °C in 5 % CO_2, 95 % air. For the cellular uptake studies, cells (2.0×10^5 cells/well) were pre-incubated in the medium for 24 h in a 24-well culture plate. After incubation, the culture medium was removed, and the cells were washed twice with HBSS. The cells were then incubated in HBSS for 10 min and incubated with D-[^{18}F]FAMT (200 kBq, final concentration; 3 μM) or L-[^{18}F]FAMT (200 kBq, final concentration; 3 μM) at 37 °C for 5, 10, 20, 30, 45, and 60 min. After the incubation, cells were washed twice with HBSS and then lysed with 500 μl of a 1 % Triton X-100 solution. The radioactivity in the cell lysate was measured by a well-type γ-counter (ARC-7001; Aloka, Tokyo, Japan). The radioactivity of each sample was normalized for the total protein concentration, which was determined using a Quick Start Protein Assay kit (Bio-Rad Laboratories, Hercules, CA, USA). For inhibition assay of cellular uptake, the cells were washed twice with HBSS or Na^+-free HBSS [137 mM choline chloride, 5.3 mM KC1, 1.3 mM $CaCl_2$, 0.49 mM $MgCl_2$, 0.41 mM $MgSO_4$, 0.35 mM K_2HPO_4, 0.44 mM KH_2PO_4, 4.2 mM $KHCO_3$, 5.6 mM D-glucose (pH 7.4)] after pre-incubation. L-Tyrosine, α-methyl-L-tyrosine, BCH and MeAIB were dissolved in 1 % DMSO/HBSS or 1 % DMSO/Na^+-free HBSS at a concentration of 1 mM. Then, the cells were incubated in HBSS or Na^+-free HBSS for 10 min and treated with 0.1 % DMSO (vehicle), 100 μM of L-tyrosine, α-methyl-L-tyrosine, BCH, or MeAIB for 10 min before addition of D-[^{18}F]FAMT [23]. At 30 min after treatment with D-[^{18}F]FAMT (200 kBq, final concentration; 3 μM), cells were washed with HBSS or Na^+-free HBSS and dissolved in 1 % Triton X-100. The radioactivity of the lysate was measured by a well-type γ-counter.

Reverse transcription polymerase chain reaction (RT-PCR)

Total RNA was isolated from cells using a Fast Pure RNA kit (Takara Bio, Shiga, Japan). The first-strand complement DNA was synthesized from 0.5 μg of total RNA with PrimeScript Reverse Transcriptase (Takara Bio). The sequences of the specific primers for LAT1, the heavy chain of 4F2 cell-surface antigen (4F2hc), which associates with LAT1 for its functional form [16], and glyceraldehyde-3-phosphate dehydrogenase (GAPDH) are shown

Table 1 RT-PCR primers

Accession no.	Primer sequences	Expected size (bp)
LAT1		
AB018009	Sense: ATTGTGCTGGCATTATACAGCGGC	271
	Antisense: AGGATGTGAACAGGGACCCATTGA	
4F2hc		
AB018010	Sense: AGCCGAGAAGAATGGTCTGGTGAA	423
	Antisense: AGCAAGTCAGTCTGAGCGACATCA	
GAPDH		
BC083511	Sense: TCATGACCACAGTCCATGCCATCA	450
	Antisense: CCCTGTTGCTGTAGCCAAATTCGT	

in Table 1. The PCR analysis was performed by first incubating each complement DNA sample with the primers (0.5 μM each), Blend *Taq* polymerase (1.25 U: Toyobo, Osaka, Japan), and deoxynucleotide mix (0.2 mM each: Toyobo). Amplification was carried out for 35 cycles (95 °C for 30 s, annealing at 60 °C for 30 s, 72 °C for 1 min). The products were then subjected to 2 % agarose gel electrophoresis. Bands were stained with ethidium bromide and photographed.

Immunoblotting

For preparation of in vitro samples, LS180 cells were dissolved in sample buffer (25 % glycerol, 1 % SDS, 62.5 mM Tris–Cl, 10 mM dithiothreitol) and incubated at 65 °C for 15 min. For preparation of in vivo samples, the tumor tissue was excised after the attenuation of radioactivity and minced. Approximately 40 mg of the tumor was dissolved in lysis buffer [20 mM Tris–HCl (pH 7.5), 150 mM NaCl, 1 mM Na_2EDTA, 1 mM EGTA, 1 % Triton, 2.5 mM sodium pyrophosphate, 1 mM β-glycerophosphate, 1 mM Na_3VO_4, 1 μg/ml leupeptin). After 1 h incubation on ice, the samples were centrifuged at 15,000 rpm for 30 min. The supernatant was mixed with 2× sample buffer (50 % glycerol, 2 % SDS, 125 mM Tris–Cl, 20 mM dithiothreitol) and incubated at 65 °C for 15 min. Aliquots of samples containing 40 μg of protein were analyzed by 10 % SDS-polyacrylamide gel electrophoresis and transferred onto a polyvinylidene difluoride membrane. Blots were incubated at 4 °C overnight in 10 mM Tris–HCl, 100 mM NaCl, 0.1 % Tween 20, pH 7.5 (TBST), with 5 % skim milk, and then with rabbit anti-LAT1 N-terminus antibody (1:5,000) at 4 °C overnight [24]. After TBST wash, the blots were incubated with goat horseradish peroxidase (HRP)-conjugated anti-rabbit IgG antibody (1:20,000; Cell Signaling Technology, Beverly, MA, USA) for 1.5 h at room temperature. The blots were again washed with TBST, and specific proteins were visualized with enhanced chemiluminescence western blotting detection reagents (GE Healthcare, Piscataway, NJ, USA).

Biodistribution studies

For the biodistribution studies in tumor-bearing mice, LS180 cells (5×10^6 cells/head) were implanted into the flanks of BALB/c nude mice. When palpable tumors developed, D-[^{18}F]FAMT (200 kBq) or L-[^{18}F]FAMT (200 kBq) in 100 μl of saline was injected into the tail veins of the mice. At selected time points after administration, the mice were euthanized, and the tissues of interest were dissected and weighed. The radioactivity was measured by a well-type γ-counter. Uptake of the tracers was expressed as a percentage of injected dose/gram of tissue.

PET imaging

PET imaging was performed using an animal PET scanner (Inveon, Siemens, Knoxville, TN, USA). L-[^{18}F]FAMT (10 MBq) was injected intravenously into the mice-bearing LS180 tumors, and imaging was performed 30 min, 1 h, and 2.5 h later. One day after the L-[^{18}F]FAMT-PET study, D-[^{18}F]FAMT (10 MBq) was injected intravenously into the mice, and imaging was performed 30 min, 1 h, and 2.5 h later. Mice were anesthetized with isoflurane (1.5 % isoflurane/98.5 % air, flow: 1.5 L/min) prior to the PET scan. Each PET scan with L-[^{18}F]FAMT or D-[^{18}F]FAMT was performed for 15 min. For the inhibition study, BCH and α-methyl-L-tyrosine were dissolved in 0.3 M HCl/saline at concentrations of 125 and 100 mM, respectively. Then 130 μl of 0.3 M HCl/saline, BCH (100 mg/kg), or α-methyl-L-tyrosine (100 mg/kg) was injected intravenously into tumor-bearing mice under anesthesia with isoflurane (1.5 % isoflurane/98.5 % air, flow: 1.5 L/min) 10 min before the administration of D-[^{18}F]FAMT. Then tumor-to-muscle ratios were calculated to analyze the inhibitory effects induced by BCH or α-methyl-L-tyrosine semi-quantitatively. For analysis of the image, a region of interest around the tumor or muscle was manually marked on the PET image and radioactivity was quantified using ASIPro VM software (CTI Concorde Microsystems, Knoxville, TN, USA).

Statistical analysis

Results are expressed as mean ± SD. The significance of differences was determined by a one-way analysis of variance, followed by Bonferroni's test for multigroup comparisons. Student's *t* test was used for two-group comparisons. The criterion of significance was $P < 0.05$, as determined with GraphPad Prism 4 software (Graph Pad Software, San Diego, CA, USA).

Results

Radiolabeling

The radiolabeling yield of D-[^{18}F]FAMT was approximately 10 %, similar to that of L-[^{18}F]FAMT. In the HPLC analysis with the LiChrosorb RP-18 column, the retention times of D-[^{18}F]FAMT and the major byproduct, 2-[^{18}F]fluoro-α-methyl-D-tyrosine (D-2-[^{18}F]FAMT), were 4.3 and 3.9 min, respectively. To avoid contamination by D-2-[^{18}F]FAMT, we discarded product that corresponds to the first half of the D-[^{18}F]FAMT peak by HPLC, achieving radiochemical purity of 96–99 % without D-2-[^{18}F]FAMT (Fig. 1). In the HPLC analysis with a chiral column, the retention times of D-[^{18}F]FAMT and L-[^{18}F]FAMT were different, and no enantiomeric contamination of each of D- and L-[^{18}F]FAMT preparation was observed (Fig. 1c, f). The specific activities of both D-[^{18}F]FAMT and L-[^{18}F]FAMT were over 120 GBq/mmol.

Stability of D-[^{18}F]FAMT and L-[^{18}F]FAMT

Over 95 % of D- and L-[^{18}F]FAMT remained intact until 6 h after incubation in murine or human plasma, indicating that both were stable in plasma. Furthermore, over 95 % of both D- and L-[^{18}F]FAMT remained intact at 60 min after administration to mice, indicating that both were also stable in vivo.

Cellular uptake studies

As shown in Fig. 2a, L-[^{18}F]FAMT immediately accumulated in LS180 cells until 10 min after addition, and reached the plateau. D-[^{18}F]FAMT accumulated more gradually in the LS180 cells, and the total amount of D-[^{18}F]FAMT in the LS180 cells was significantly lower than that of L-[^{18}F]FAMT. To investigate the mechanism of cellular uptake, the uptake of D-[^{18}F]FAMT was competitively inhibited with selective inhibitors of amino acid

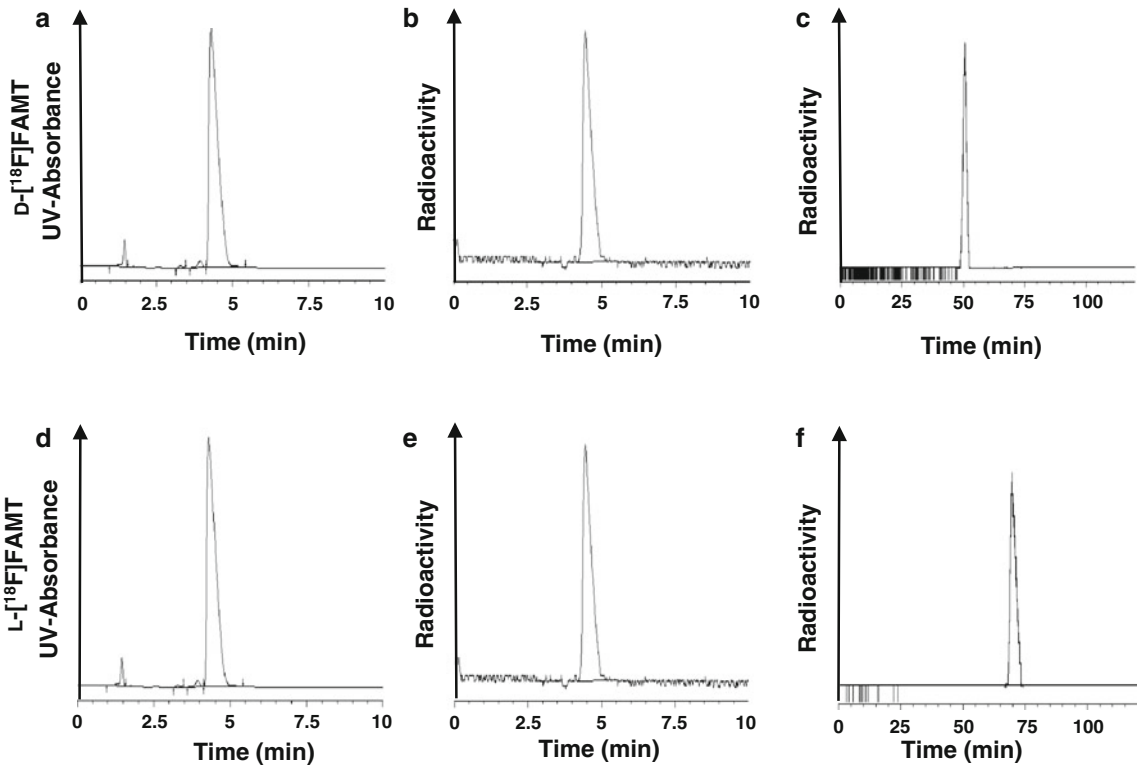

Fig. 1 HPLC profiles of D- and L-[^{18}F]FAMT. Analytical HPLC profiles of standard of FAMT (**a**, **d**) and [^{18}F]FAMT (**b**, **e**). HPLC profiles after enantiomeric analysis of D-[^{18}F]FAMT (**c**) or L-[^{18}F]FAMT (**f**)

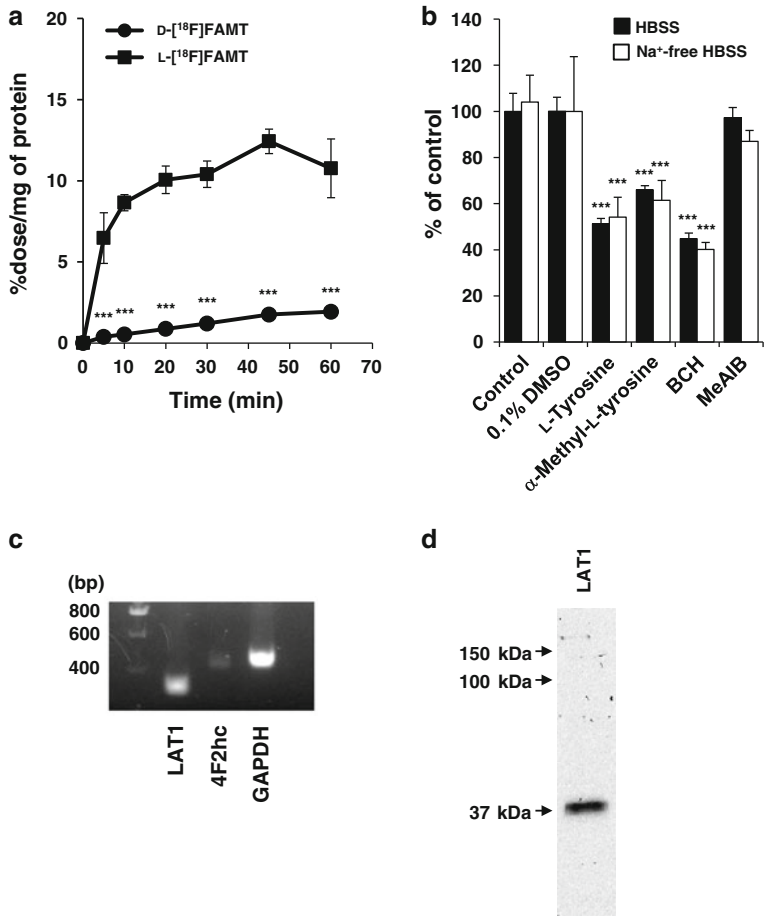

Fig. 2 Cellular uptake of D-[^{18}F]FAMT was regulated by LAT1. **a** Cellular uptake of D- and L-[^{18}F]FAMT was determined at various time points. A statistically significant difference between D-[^{18}F]FAMT and L-[^{18}F]FAMT is indicated by $***P < 0.001$. **b** Cells were pretreated with 0.1 % DMSO (vehicle), L-tyrosine (100 μM), α-methyl-L-tyrosine (100 μM), BCH (100 μM), and MeAIB (100 μM) for 10 min in HBSS or Na^+-free HBSS. At 30 min after incubation with D-[^{18}F]FAMT, cells were lysed and the radioactivity was determined. A statistically significant difference from the control is indicated by $***P < 0.001$. **c** Expression of LAT1 and 4F2hc mRNA in LS180 cells was determined by RT-PCR. Representative images from three independent experiments are shown. GAPDH was simultaneously detected as a control. **d** Expression of LAT1 protein in LS180 cells was determined by immunoblotting. A representative image from three independent experiments is shown

transporter in HBSS or Na^+-free HBSS. The uptake of D-[^{18}F]FAMT was significantly inhibited by pretreatment with 100 μM of L-tyrosine, α-methyl-L-tyrosine (a selective inhibitor of LAT1) [18, 24], and BCH (a selective inhibitor of system L) (Fig. 2b). The uptake was not inhibited by pretreatment with 100 μM of MeAIB (a selective inhibitor of system A). No difference of cellular uptake between HBSS and Na^+-free HBSS was observed. RT-PCR analysis showed that both LAT1 and 4F2hc were expressed in LS180 cells, and the expression level of LAT1 was high (Fig. 2c). The expression of LAT1 protein was also examined by immunoblotting (Fig. 2d). Only one band with a molecular weight of approximately 38 kDa, corresponding to LAT1, was detected. These results indicate that D-[^{18}F]FAMT was transported into LS180 cells through LAT1.

Biodistribution studies in LS180-bearing mice

As shown in Table 2, D-[^{18}F]FAMT showed rapid clearance from the blood, marked accumulation and retention in the tumor, and low accumulation in the non-target organs. However, the level of accumulation of D-[^{18}F]FAMT in the tumor was lower than that of L-[^{18}F]FAMT. The radioactivity of D-[^{18}F]FAMT in the kidney and pancreas was reduced to levels similar to the other normal organs by 3 h after administration, while the radioactivity of L-[^{18}F]FAMT in the kidney and pancreas was retained and remained elevated at 3 h after administration as opposed to that of the other normal organs. The tumor-to-blood and tumor-to-muscle ratios of D-[^{18}F]FAMT were similar to those of L-[^{18}F]FAMT at every time point, while tumor-to-kidney

Table 2 Biodistribution of D-[^{18}F]FAMT and L-[^{18}F]FAMT in tumor-bearing mice

	30 min	1 h	3 h
D-[^{18}F]FAMT			
Blood	0.79 ± 0.12	0.27 ± 0.10	0.00 ± 0.00
Liver	1.47 ± 0.36	0.58 ± 0.03	0.02 ± 0.01
Kidney	3.87 ± 1.59	1.39 ± 0.21	0.15 ± 0.08
Intestine	0.47 ± 0.04	0.33 ± 0.10	0.27 ± 0.04
Pancreas	3.41 ± 1.03	2.24 ± 0.48	0.16 ± 0.15
Stomach	0.26 ± 0.11	0.01 ± 0.02	0.00 ± 0.00
Muscle	0.44 ± 0.21	0.42 ± 0.28	0.24 ± 0.21
Tumor	1.13 ± 0.32	1.14 ± 0.31	0.67 ± 0.12
Tumor-to-blood ratio	1.45 ± 0.47	4.35 ± 0.82	–
Tumor-to-muscle ratio	3.19 ± 1.96	3.72 ± 2.36	2.12 ± 0.46
Tumor-to-kidney ratio	0.31 ± 0.11*	0.81 ± 0.14***	5.46 ± 3.02*
Tumor-to-pancreas ratio	0.33 ± 0.04	0.50 ± 0.03	2.65 ± 0.25*
L-[^{18}F]FAMT			
Blood	2.56 ± 0.45	0.92 ± 0.23	0.07 ± 0.07
Liver	2.63 ± 0.34	1.11 ± 0.30	0.14 ± 0.02
Kidney	60.48 ± 9.43	25.23 ± 5.61	4.20 ± 0.42
Intestine	1.94 ± 0.43	0.91 ± 0.15	0.13 ± 0.01
Pancreas	17.12 ± 3.74	8.61 ± 1.29	0.92 ± 0.14
Stomach	0.58 ± 0.08	0.60 ± 0.36	0.14 ± 0.11
Muscle	1.75 ± 0.52	1.36 ± 0.19	0.53 ± 0.08
Tumor	5.91 ± 0.54	4.55 ± 0.48	1.36 ± 0.36
Tumor-to-blood ratio	2.37 ± 0.51	5.13 ± 1.17	13.13 ± 3.92
Tumor-to-muscle ratio	3.61 ± 1.06	3.37 ± 0.25	2.54 ± 0.36
Tumor-to-kidney ratio	0.10 ± 0.02	0.19 ± 0.05	0.33 ± 0.12
Tumor-to-pancreas ratio	0.36 ± 0.07	0.53 ± 0.05	1.47 ± 0.30

Each value represents the mean % injected dose per gram of tissue ± SD of three or four animals. A statistically significant difference of tumor-to-kidney ratio and tumor-to-pancreas ratio between D-[^{18}F]FAMT and L-[^{18}F]FAMT is indicated by * ($P < 0.05$) or *** $P < 0.001$

and tumor-to-pancreas ratios of D-[^{18}F]FAMT were significantly higher than those of L-[^{18}F]FAMT.

PET imaging

Corresponding to the results of the biodistribution study, retention of D-[^{18}F]FAMT in the kidney was low (Fig. 3). High radioactivity was observed in the bladder after administration of L- or D-[^{18}F]FAMT, indicating that both tracers were excreted from the kidney to the urine. The implanted tumor was visualized by PET with both

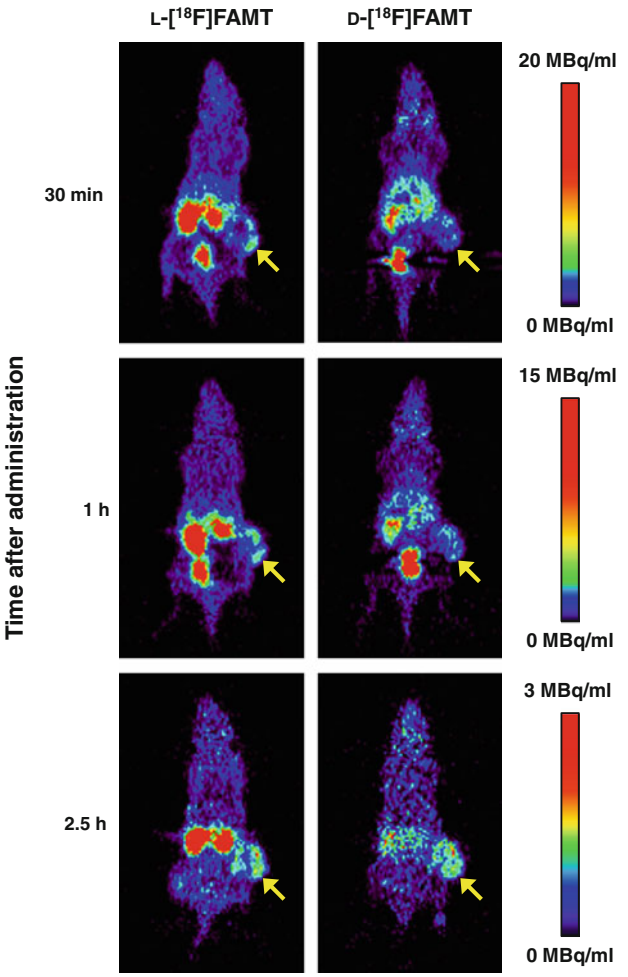

Fig. 3 PET images of LS180-bearing mice with D-[^{18}F]FAMT (10 MBq) and L-[^{18}F]FAMT (10 MBq) in isoflurane-anesthetized mice. Mice were imaged at 30 min, 1, and 2.5 h after intravenous injection of each PET tracer. Representative coronal sections at each time point are shown. *Arrows* indicate the position of the implanted tumor. The *calibration bar* is shown at the *right side* of the images

D-[^{18}F]FAMT and L-[^{18}F]FAMT. Although the tumor-to-background contrast of both tracers was similar until 1 h after administration, tumor-to-background contrast of D-[^{18}F]FAMT became higher than L-[^{18}F]FAMT at 2.5 h after administration. As shown in Fig. 4a, the accumulation of D-[^{18}F]FAMT in the tumor was decreased by pretreatment with BCH (100 mg/kg) or α-methyl-L-tyrosine (100 mg/kg). The absolute accumulation of radioactivity in the tumor was significantly decreased by administration of BCH in comparison with administration of control, and while the radioactivity in the tumor was increased by pretreatment with α-methyl-L-tyrosine, the radioactivity in muscle, which was measured as a background, was also increased. Since body clearance of radioactivity seemed to be slowed by pretreatment with α-methyl-L-tyrosine, radioactivity level would increase in the organs and the tumor. Semi-quantitative analysis showed that the ratio of

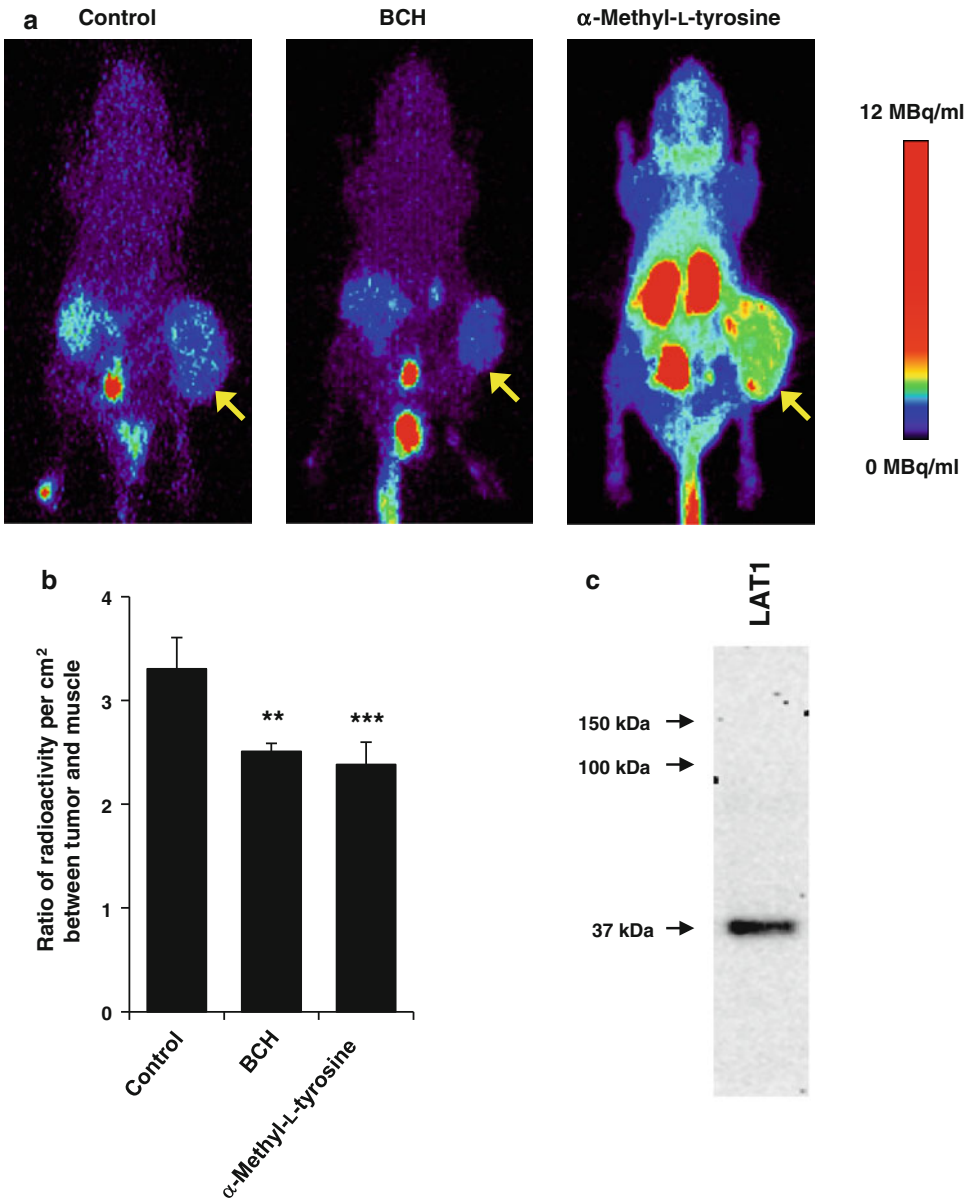

Fig. 4 Involvement of LAT1 in tumor uptake of D-[^{18}F]FAMT in vivo. **a** Mice were pretreated with vehicle (control: 0.3 M HCl/saline), BCH (100 mg/kg), and α-methyl-L-tyrosine (100 mg/kg) for 10 min, and scanned at 2.5 h after intravenous injection of D-[^{18}F]FAMT. Representative projection images are shown. *Arrows* indicate the position of the implanted tumor. The *calibration bar* is shown at the *right side* of the images. **b** The effect of inhibitors was semi-quantitatively determined by calculating the ratio of radioactivity per cm^2 between the tumor and muscle (control, $n = 5$; BCH, $n = 4$; α-methyl-L-tyrosine, $n = 3$). A statistically significant difference from control is indicated by $^{**}P < 0.01$ or $^{***}P < 0.001$. **c** Expression of LAT1 protein in tumors isolated from LS180-bearing mice was determined by immunoblotting. A representative image from three independent experiments is shown

D-[^{18}F]FAMT radioactivity per cm^2 between tumor and muscle was significantly decreased by the administration of both inhibitors (Fig. 4b). LAT1 expression was also observed in the implanted tumor (Fig. 4c), indicating that D-[^{18}F]FAMT was also accumulated in the tumor through LAT1 in vivo.

Discussion

Since L-[^{18}F]FAMT accumulates in tumors more selectively than [^{18}F]FDG, it is used for the detection of various types of human neoplasm [6, 7, 25]. Recently, amino acid tracers using D-isomers have been developed, which could reduce radioactivity in non-target organs and provide clear images of tumors [22], and we proposed that the D-isomer of [^{18}F]FAMT could show rapid blood clearance and low accumulation in non-target organs, consequently achieving clear image of tumors early after administration. In our experiments, D-[^{18}F]FAMT was prepared by radiolabeling of α-methyl-D-tyrosine with ^{18}F according to the published method for synthesis of L-[^{18}F]FAMT [6]. In general, high enantiomeric purity is required for the comparison of optical isomers. It has been reported that the enantiomeric purity is affected by radiolabeling conditions such as temperature and pH [26, 27]. Enantiomeric analysis of ^{18}F-labeled D- or L-FAMT showed only one peak, which correspond to D- or L-[^{18}F]FAMT, and no enantiomeric contamination was observed. Thus, we confirmed that D- or L-[^{18}F]FAMT was

successfully synthesized without racemization in this study.

L-[^{18}F]FAMT is transported into tumor cells solely through the amino acid transport system, and in particular, involvement of LAT1 has been suggested [10, 13–15]. In our results, expressions of both LAT1 and 4F2hc were observed in LS180 cells, and cellular uptake of D-[^{18}F]FAMT was significantly inhibited by pretreatment with selective inhibitor of LAT1 in Na^+-free HBSS. The expression of LAT1 was also confirmed in vivo in the implanted tumor, and the accumulation of D-[^{18}F]FAMT in the tumor tissue was significantly inhibited with selective inhibition of LAT1. Therefore, our results suggest major involvement of LAT1 in the uptake of D-[^{18}F]FAMT into tumor tissues.

In the biodistribution study, D-[^{18}F]FAMT was rapidly cleared from the blood, and the amounts of D-[^{18}F]FAMT retained in the kidney and pancreas were much lower than that of L-[^{18}F]FAMT. This rapid blood clearance would be due to D-isomerism, since D-[^{18}F]FAMT, similar to L-[^{18}F]FAMT, remained intact in the blood after administration in mice. In the kidney, L-amino acids are reabsorbed from the proximal tubule by various transporters, including amino acid transporters, after glomerular filtration [28]. However, D-amino acids are rarely reabsorbed from the proximal tubule because of low affinity to the transporters [29] and are mainly excreted in the urine [20, 29, 30]. Thus, low reabsorption of D-[^{18}F]FAMT from the proximal tubule would cause low radioactivity in the kidney and rapid blood clearance. In inhibition study, body clearance of radioactivity seemed to be slowed only by pretreatment with α-methyl-L-tyrosine, suggesting that α-methyl-L-tyrosine would inhibit renal excretion of D-[^{18}F]FAMT. It has been reported that α-methyl-L-tyrosine is excreted from kidney to urine without metabolism [31]. Thus, renal transport system of D-[^{18}F]FAMT might be competitively inhibited by administration of large amounts of α-methyl-L-tyrosine. Previously, Shikano et al. [32, 33] have shown an accumulation of 3-iodo-α-methyl-L-tyrosine, an iodine-labeled analog of L-[^{18}F]FAMT, in the renal cortex and suggested involvement of tubular secretion with amino acids transport systems including organic anion transporters in the proximal tubular epithelial cells. Thus, α-methyl-L-tyrosine might inhibit transporters which are involved in the tubular secretion of D-[^{18}F]FAMT, followed by the retention of radioactivity in the body.

PET imaging using D-[^{18}F]FAMT did not allow clear visualization of tumor early after administration. However, D-[^{18}F]FAMT did allow more selective and clearer visualization of tumors by PET at later time points compared to L-[^{18}F]FAMT. A lower radiation burden from D-[^{18}F]FAMT than from L-[^{18}F]FAMT can also be expected because of the rapid blood clearance and lower accumulation of D-[^{18}F]FAMT in the non-target organs. These results suggest potential of D-[^{18}F]FAMT as a novel amino acid tracer for PET. Whereas, since accumulation of D-[^{18}F]FAMT in the tumor was lower than that of L-[^{18}F]FAMT, the sensitivity of tumor detection with D-[^{18}F]FAMT would be low. Decreasing of the sensitivity could not be critical faults in the D-[^{18}F]FAMT-PET since D-[^{18}F]FAMT will be used for the definitive diagnosis of the tumor which has been already detected by [^{18}F]FDG-PET, however, large amounts of D-[^{18}F]FAMT would be required to obtain clear image in some clinical cases. It would be difficult to supply enough amount of D-[^{18}F]FAMT by current method to carry out PET in routine clinical practice. Therefore, improvement of D-[^{18}F]FAMT synthesis would be important to apply D-[^{18}F]FAMT to clinical diagnosis.

In vitro evaluations also showed that cellular uptake of D-[^{18}F]FAMT was slow, and the total amount of D-[^{18}F]FAMT in the LS180 cells was significantly lower than that of L-[^{18}F]FAMT. It has been reported that there are two interactions involved in L-amino acid recognition by LAT1, the electronic interaction of positive and negative charges at the α-carbon, and the hydrophobic interaction between the substrate side chain and the substrate binding site of LAT1 [18]. Considering these mechanisms of substrate recognition by LAT1, we speculated that both interactions would be difficult with the D-isomers because of the conformational differences, reducing the affinity with LAT1 for D-amino acids, and resulting in low uptake of D-[^{18}F]FAMT into LS180 cells and the corresponding low uptake of D-[^{18}F]FAMT in the tumor [29]. Consequently, the tumor-to-blood and tumor-to-muscle ratios were similar to those of L-[^{18}F]FAMT at every time point after injection in mice, although the blood clearance of D-[^{18}F]FAMT was much more rapid than that of L-[^{18}F]FAMT.

Our results also demonstrated a reduction of radioactivity in the kidney and pancreas, leading to elevation of both the tumor-to-kidney and tumor-to-pancreas ratios (D-[^{18}F]FAMT tumor-to-kidney ratio 5.46 ± 3.02, tumor-to-pancreas ratio 2.65 ± 0.25 at 3 h; L-[^{18}F]FAMT tumor-to-kidney ratio 0.33 ± 0.12, tumor-to-pancreas ratio 1.47 ± 0.30 at 3 h). Since LAT1 is highly expressed in renal and pancreatic cancers, these cancers could be the possible targets of amino acid tracers [34, 35]. It is still difficult to image renal or pancreatic cancers with existing amino acid tracers because of high accumulation in normal renal or pancreatic tissues. Therefore, the low baseline accumulation in the kidney or pancreas observed in this study indicates that D-[^{18}F]FAMT could be a novel amino acid tracer that is useful for PET imaging of renal or pancreatic neoplasms.

In the present study, D-[^{18}F]FAMT showed rapid clearance from the blood and reduced radioactivity in non-target organs. Furthermore, our results showed that D-[^{18}F]FAMT is highly stable both in vitro and in vivo and that it is transported into the tumor via LAT1. Although PET imaging with D-[^{18}F]FAMT did not give a clearer image of the tumor early after administration, as had been anticipated, the D-[^{18}F]FAMT did provide higher tumor-to-background contrast and lower exposure dose to patients than L-[^{18}F]FAMT. These results suggest that D-[^{18}F]FAMT could potentially serve as a novel PET tracer for imaging of malignant tumors which has high expression of LAT1.

Acknowledgments This work was supported by Funding Program for Next Generation World-Leading Researchers (NEXT program) from Cabinet Office, Government of Japan. We are grateful to Mr. Takashi OGASAWARA for operation of the biomedical cyclotron. We also would like to thank the staff of the Medical Radioisotope Application Group at the Japan Atomic Energy Agency as well as the Departments of Diagnostic Radiology and Nuclear Medicine at Gunma University Graduate School of Medicine for their cooperation and helpful input.

References

1. Plathow C, Weber WA. Tumor cell metabolism imaging. J Nucl Med. 2008;49(Suppl 2):43S–63S.
2. Zhu A, Shim H. Current molecular imaging positron emitting radiotracers in oncology. Nucl Med Mol Imaging. 2011;45:1–14.
3. Jager PL, Vaalburg W, Pruim J, de Vries EG, Langen KJ, Piers DA. Radiolabeled amino acids: basic aspects and clinical applications in oncology. J Nucl Med. 2001;42:432–45.
4. Långström B, Antoni G, Gullberg P, Halldin C, Malmborg P, Någren K, et al. Synthesis of L- and D-[methyl-^{11}C]methionine. J Nucl Med. 1987;28:1037–40.
5. Wester HJ, Herz M, Weber W, Heiss P, Senekowitsch-Schmidtke R, Schwaiger M, et al. Synthesis and radiopharmacology of O-(2-[^{18}F]fluoroethyl)-L-tyrosine for tumor imaging. J Nucl Med. 1999;40:205–12.
6. Tomiyoshi K, Amed K, Muhammad S, Higuchi T, Inoue T, Endo K, et al. Synthesis of isomers of ^{18}F-labelled amino acid radiopharmaceutical: position 2- and 3-L-^{18}F-alpha-methyltyrosine using a separation and purification system. Nucl Med Commun. 1997;18:169–75.
7. Inoue T, Tomiyoshi K, Higuichi T, Ahmed K, Sarwar M, Aoyagi K, et al. Biodistribution studies on L-3-[fluorine-18]fluoro-alpha-methyl tyrosine: a potential tumor-detecting agent. J Nucl Med. 1998;39:663–7.
8. Inoue T, Shibasaki T, Oriuchi N, Aoyagi K, Tomiyoshi K, Amano S, et al. ^{18}F Alpha-methyl tyrosine PET studies in patients with brain tumors. J Nucl Med. 1999;40:399–405.
9. Inoue T, Koyama K, Oriuchi N, Alyafei S, Yuan Z, Suzuki H, et al. Detection of malignant tumors: whole-body PET with fluorine 18 alpha-methyl tyrosine versus FDG—preliminary study. Radiology. 2001;220:54–62.
10. Kaira K, Oriuchi N, Otani Y, Shimizu K, Tanaka S, Imai H, et al. Fluorine-18-alpha-methyltyrosine positron emission tomography for diagnosis and staging of lung cancer: a clinicopathologic study. Clin Cancer Res. 2007;13:6369–78.
11. Miyakubo M, Oriuchi N, Tsushima Y, Higuchi T, Koyama K, Arai K, et al. Diagnosis of maxillofacial tumor with L-3-[^{18}F]-fluoro-alpha-methyltyrosine (FMT) PET: a comparative study with FDG-PET. Ann Nucl Med. 2007;21:129–35.
12. Kaira K, Oriuchi N, Shimizu K, Ishikita T, Higuchi T, Imai H, et al. Evaluation of thoracic tumors with ^{18}F-FMT and ^{18}F-FDG PET-CT: a clinicopathological study. Int J Cancer. 2009;124:1152–60.
13. Kaira K, Oriuchi N, Imai H, Shimizu K, Yanagitani N, Sunaga N, et al. Prognostic significance of L-type amino acid transporter 1 expression in resectable stage I–III nonsmall cell lung cancer. Br J Cancer. 2008;98:742–8.
14. Kaira K, Oriuchi N, Shimizu K, Imai H, Tominaga H, Yanagitani N, et al. Comparison of L-type amino acid transporter 1 expression and L-[3-^{18}F]-α-methyl tyrosine uptake in outcome of non-small cell lung cancer. Nucl Med Biol. 2010;37:911–6.
15. Wiriyasermkul P, Nagamori S, Tominaga H, Oriuchi N, Kaira K, Nakao H, et al. Transport of 3-fluoro-L-α-methyL-tyrosine by tumor-upregulated L-type amino acid transporter 1: a cause of the tumor uptake in PET. J Nucl Med. 2012;53:1253–61.
16. Kanai Y, Segawa H, Miyamoto K, Uchino H, Takeda E, Endou H. Expression cloning and characterization of a transporter for large neutral amino acids activated by the heavy chain of 4F2 antigen (CD98). J Biol Chem. 1998;273:23629–32.
17. Yanagida O, Kanai Y, Chairoungdua A, Kim DK, Segawa H, Nii T, et al. Human L-type amino acid transporter 1 (LAT1): characterization of function and expression in tumor cell lines. Biochim Biophys Acta. 2001;1514:291–302.
18. Uchino H, Kanai Y, Kim DK, Wempe MF, Chairoungdua A, Morimoto E, et al. Transport of amino acid-related compounds mediated by L-type amino acid transporter 1 (LAT1): insights into the mechanisms of substrate recognition. Mol Pharmacol. 2002;61:729–37.
19. Imai H, Kaira K, Oriuchi N, Shimizu K, Tominaga H, Yanagitani N, et al. Inhibition of L-type amino acid transporter 1 has antitumor activity in non-small cell lung cancer. Anticancer Res. 2010;30:4819–28.
20. Crampton RF, Smyth DH. The excretion of the enantiomorphs of aminoacids. J Physiol. 1953;122:1–10.
21. Doolan PD, Harper HA, Hutchin ME, Shreeve WW. Renal clearance of eighteen individual amino acids in human subjects. J Clin Invest. 1955;34:1247–55.
22. Tsukada H, Sato K, Fukumoto D, Nishiyama S, Harada N, Kakiuchi T. Evaluation of D-isomers of O-^{11}C-methyl tyrosine and O-^{18}F-fluoromethyl tyrosine as tumor-imaging agents in tumor-bearing mice: comparison with L- and D-^{11}C-methionine. J Nucl Med. 2006;47:679–88.
23. Ohshima Y, Hanaoka H, Watanabe Sh, Sugo Y, Watanabe Sa, Tominaga H, et al. Preparation and biological evaluation of 3-[^{76}Br]bromo-α-methyl-L-tyrosine, a novel tyrosine analog for positron emission tomography imaging of tumors. Nucl Med Biol. 2011;38:857–65.
24. Morimoto E, Kanai Y, Kim do K, Chairoungdua A, Choi HW, Wempe MF, et al. Establishment and characterization of mammalian cell lines stably expressing human L-type amino acid transporters. J Pharmacol Sci. 2008;108:505–16.
25. Kaira K, Oriuchi N, Sunaga N, Ishizuka T, Shimizu K, Yamamoto N. A systemic review of PET and biology in lung cancer. Am J Transl Res. 2011;3:383–91.
26. Ishiwata K, Kasahara C, Hatano K, Ishii S, Senda M. Carbon-11 labeled ethionine and propionine as tumor detecting agents. Ann Nucl Med. 1997;11:115–22.
27. Ishiwata K, Ido T, Vaalburg W. Increased amounts of D-enantiomer dependent on alkaline concentration in the synthesis of L-[methyl-^{11}C]methionine. Int J Rad Appl Instrum A. 1988;39:311–4.
28. Bröer S. Amino acid transport across mammalian intestinal and renal epithelia. Physiol Rev. 2008;88:249–86.
29. Friedman M, Levin CE. Nutritional and medicinal aspects of D:-amino acids. Amino Acids. 2011. doi:10.1007/s00726-011-0915-1.

30. Young JA, Freedman BS. Renal tubular transport of amino acids. Clin Chem. 1971;17:245–66.
31. Engelman K, Jéquier E, Udenfriend S, Sjoerdsma A. Metabolism of alpha-methyltyrosine in man: relationship to its potency as an inhibitor of catecholamine biosynthesis. J Clin Invest. 1968; 47:568–76.
32. Shikano N, Kawai K, Nakajima S, Nishii R, Flores LG 2nd, Kubodera A, et al. Renal accumulation and excretion of radioiodinated 3-iodo-alpha-methyl-L-tyrosine. Ann Nucl Med. 2004;18:263–70.
33. Shikano N, Kawai K, Nakajima S, Kubodera A, Kubota N, Ishikawa N, et al. Transcellular transport of radioiodinated 3-iodo-alpha-methyl-L-tyrosine across monolayers of kidney epithelial cell line LLC-PK1. Ann Nucl Med. 2004;18:227–34.
34. Kaira K, Sunose Y, Arakawa K, Ogawa T, Sunaga N, Shimizu K, et al. Prognostic significance of L-type amino-acid transporter 1 expression in surgically resected pancreatic cancer. Br J Cancer. 2012;107:632–8.
35. Shnitsar V, Eckardt R, Gupta S, Grottker J, Muller GA, Koepsell H, et al. Expression of human organic cation transporter 3 in kidney carcinoma cell lines increases chemosensitivity to melphalan, irinotecan, and vincristine. Cancer Res. 2009;69:1494–501.